Reactive adsorption of ammonia on Cu-based MOF /graphene composites

Camille Petit, Barbara Beacom and Teresa J. Bandosz[*]

Department of Chemistry

The City College and the Graduate School of the City University of New York

160 Convent Avenue

New York, NY 10031 (USA)

Abstract

New composites based on HKUST-1 and graphene layers are tested for ammonia adsorption at room temperature in both dry and moist conditions. The materials are characterized by X-ray diffraction, FT-IR spectroscopy, adsorption of nitrogen and thermal analyses. Unlike other MOF/GO composites reported in previous studies, these materials are water stable. Ammonia adsorption capacities on the composites are higher than the ones calculated for the physical mixture of components, suggesting the presence of a synergetic effect between the MOF and graphene layers. The increased porosity and dispersive forces being the consequence of the presence of graphene layers are responsible for the enhanced adsorption. In addition to its retention via physical forces, ammonia is also adsorbed via binding to the copper sites in

[*] To whom correpondance should be addressed. Telephone: 212-650-6017. Fax: 212-650-6107. E-mail: tbandosz@ccny.cuny.edu.

HKUST-1 and then, progressively, via reaction with the MOF component. This reactive adsorption is visible through two successive changes of the adsorbents' color during the breakthrough tests. More ammonia is adsorbed in moist conditions than in dry conditions owing to its dissolution in a water film present in the pore system.

Keywords

Metal-organic framework, ammonia, graphite oxide, composite, adsorption

Introduction

Adsorption of small molecules of toxic gases, and particularly ammonia, has been the focus of intense research.[1-9] Indeed, even though many adsorbents have shown high performance and/or are commercially used in NH_3 removal, the progressive desorption of ammonia over time remains a challenging issue.[10] Activated carbons, which are among the mostly used NH_3 adsorbents, suffer from that problem. Despite their relatively high surface area (about 1000-2000 m^2/g), the small size of ammonia (3 Å)[11] as well as its low heat of adsorption on carbonaceous materials (very close to the heat of vaporization),[12, 13] enable only weak retention forces.

To overcome the above-mentioned problem, ammonia adsorbents must fulfill two conditions.[14, 15] The first one is the presence of a highly porous structure with pores similar in size to the size of ammonia in order to increase physical adsorption forces. The second important factor is the adsorbent chemistry. This includes the presence of functional groups reacting with ammonia to enable its strong retention on the adsorbent structure. The latter mechanism is often referred to as reactive adsorption.

A new class of materials, called metal-organic frameworks (MOFs), has been the subject of an intensive research in the past decade.[9, 16, 17] These compounds are formed by the self-assembly of metal ions, acting as coordination centers, with polyatomic organic bridging

ligands.[18] This results in the formation of highly porous crystalline materials.[18] Owing to the diversity of their metallic centers and organic functionalities, one can tailor materials with specific pore shape, size, volume and chemistry.[18] This feature makes these materials prime candidates for applications in gas purification, gas separation or heterogeneous catalysis.[19, 20]

Ammonia adsorption on MOF materials has been reported in a few studies.[7, 21] Britt and coworkers have tested ammonia adsorption on six different MOFs: MOF-5, MOF-177, IRMOF-62, HKUST-1 (also called MOF-199), MOF-74 and IRMOF-3 with the best performances obtained with the last three materials.[7] In the case of IRMOF-3, it was hypothesized that hydrogen bonding of ammonia with the amine functionality present on the organic ligand of this MOF was responsible for the high NH_3 adsorption capacity. On the other hand, ammonia adsorption on HKUST-1 was thought to occur via chemisorption on the open copper sites of the material.[7] The coordination of ammonia to these metallic sites was visible through a change of the adsorbent color during the breakthrough tests from dark blue/purple to light blue. This change was similar to the one observed when water binds to the copper sites.[7] However, unlike in the case of water, this color modification was irreversible upon purging in nitrogen.[7] No test on ammonia desorption was reported by Britt and coworkers to analyze the strength of the retention and no analyses were performed to verify the proposed mechanisms of adsorption.[7]

Recently, Peterson and coworkers studied the removal of ammonia on HKUST-1 via MAS NMR technique.[21] HKUST-1, contains Cu^{2+} dimers as the metallic sites linked to oxygen atoms from benzene tricarboxylate (BTC) (the organic ligand).[22] It is made of interconnected channels of square-shaped pores (9 Å by 9 Å) and its proposed chemical formula is $Cu_3(BTC)_2$.[22] Peterson and coworkers showed that ammonia adsorption on this MOF, under dry conditions, led to the formation of an intermediate diammine copper (II) complex with some remains of the original network. When ammonia breakthrough tests were performed in

the presence of water vapor, the intermediate species, $Cu(OH)_2$ and $(NH_4)_3BTC$, were found and the subsequent formation of $Cu(NH_3)_4^{2+}$ was evidenced. In both cases (humid and dry), the porosity of MOF was partially lost after exposure to NH_3 with the most pronounced decrease seen in moist conditions.[21]

Recently, composites of MOF-5 (a zinc-based MOF) and graphite oxide (GO) have been prepared and tested in ammonia adsorption.[23, 24] These materials offered higher dispersive forces than MOF alone and thus an enhancement in ammonia adsorption compared to the one calculated for the physical mixture of the two components was observed.[23, 24] This enhancement was attributed to the presence of graphene layers, which increase the physical forces in composites compared to MOF. Indeed, it has to be mentioned that physical adsorption forces in MOFs may not be strong enough to retain small molecules such as ammonia. This drawback is linked to the wide void space present in these materials.

Nevertheless, the collapse of the MOF-5 structure in the presence of humidity limited the environmental applications of the synthesized composites.[25] Therefore the formation of new water-stable composites is needed. Examples of such "water-resistant" MOF include copper-based MOFs (e.g. HKUST-1),[26, 27] a zinc-based MOF,[28] a chromium based MOF (MIL-101)[29] as well as a zeolitic imidazolate framework (ZIF-8)[29, 30]. It has to be noted that the water stability of the latter materials can take several meanings. For instance HKUST-1 is stable in a sense that the structure remains the same whether water molecules from a vapor phase are bound to the copper sites or not.[26] However, immersion of this MOF in water eventually causes its collapse, which is not the case of MIL-101 and ZIF-8.[29] Finally, other MOFs are stable only in the presence of water and loose their porosity reversibly upon dehydration.[27, 28] In a recent study, we have described the successful formation of new MOF/GO composites with HKUST-1 as the water-stable MOF component.[31] The increased porosity of the

composites compared to the parent materials as well as the known affinity of ammonia for copper,[32] make these materials potential adsorbents for ammonia.

Therefore, the objective of this study is to test these new composites as adsorbents of ammonia and to characterize the mechanisms of the retention process. Their filtration performances are discussed and compared to the ones of the parent materials.

Materials and Methods

Materials

The synthesis of the parent materials, referred to as HKUST-1 and GO, can be found in Ref [23]. It was done following the syntheses described by Millward and coworkers[33] for HKSUT-1 and Seredych and Bandosz[34] for GO. In Ref [31], the preparation of the composites whose GO content ranges from 5 to 46 wt % of the final material weight (5, 9, 18, 38, and 46 wt %) is also described. The composites are referred to as MG-n with n=1, 2, 3, 4 and 5, for the different GO contents (5, 9, 18, 38, and 46 wt %, respectively).

NH_3 breakthrough dynamic test

In order to determine the ammonia breakthrough capacity, dynamic breakthrough tests were performed at room temperature. In a typical test, a flow of ammonia diluted with air went through a fixed bed of adsorbent with a total inlet flow rate of 225 mL/min and an ammonia concentration of 1000 ppm. The adsorbent's bed contained about 2 cm^3 of glass beads well mixed with the amount of adsorbent required to obtain a homogeneous bed (between 50 and 120 mg). The mixture was packed into a glass column. The beads were used to avoid the pressure drop and thus to favor the kinetics of the breakthrough tests. The concentration of ammonia in the outlet gas was measured using an electrochemical sensor (Multi-Gas Monitor ITX system). The adsorption capacity of each adsorbent was calculated in mg per g of sorbent

by integration of the area above the breakthrough curve. Tests in dry and wet conditions were implemented by diluting the ammonia stream with either dry or moist air stream, respectively. This was done to analyze the effects of water on the adsorption capacity. In another series of test, the adsorbents were subjected to a flow of moist air only for 30 minutes. This prehumidification step was followed by a breakthrough test in dry conditions. After the breakthrough tests, all samples were exposed to a flow of carrier air only (180 mL/min) to impose the desorption of ammonia and thus to evaluate the strength of its retention. The suffixes –ED and -EM are added to the name of the samples after exposure to ammonia in dry and moist conditions, respectively.

XRD

X-ray diffraction (XRD) measurements were conducted using standard powder diffraction procedures. Adsorbents (initial and exhausted) were ground with DMF (methanol for GO) in a small agate mortar. The mixture was smear-mounted onto a glass slide and then analyzed by Cu_{Ka} radiation generated in a Philips X'Pert X-ray diffractometer. A diffraction experiment was run on standard glass slide for the background correction.

Thermal analysis

Thermogravimetric (TG) curves and their derivatives (DTG) were obtained using a TA Instrument thermal analyzer. The samples (initial and exhausted) were heated from 30 to 1000 ^{o}C with a heating rate of 10 deg/min under a flow of nitrogen held at 100 mL/min.

FT-IR spectroscopy

Fourier transform infrared (FT-IR) spectroscopy was carried out using a Nicolet Magna-IR 830 spectrometer using the attenuated total reflectance method (ATR). The spectrum was

generated, collected 16 times and corrected for the background noise. The experiments were done on the powdered samples (initial and exhausted), without KBr addition.

pH

The pH of the samples before exposure to NH_3 was measured. The adsorbent powder (about 0.1g) was stirred overnight with distilled water (5 mL) and then the pH of the suspension was recorded.

Sorption of nitrogen

Nitrogen isotherms of the samples were measured at 77 K using an ASAP 2010 (Micromeritics). Prior to each measurement, samples were outgassed at 120 ^{o}C. Approximately 0.10 g of sample was used for these analyses. The surface area, S_{BET}, (BET method), the micropore volume, V_{mic}, (Dubinin-Radushkevitch method)[35], the mesopore volume, V_{mes}, the total pore volume, V_t, were calculated from the isotherms.

Results and Discussion

Measured ammonia breakthrough and desorption curves in both dry and moist conditions are presented in Figure 1. Table 1 lists the adsorption capacities calculated from the breakthrough curves. When analyzing the breakthrough curves, one has to remember that the mass of adsorbent taken to prepare the bed varies from one material to another (between 50 and 120 mg). That is why the breakthrough curves have been plotted in min/g and not min as it is often the case in order to allow a direct comparison in terms of capacity between the different samples. Moreover, it is interesting to study the shape of the curves. In dry conditions, steep breakthrough and desorption curves are observed for all materials suggesting the fast kinetics of adsorption and the strong retention of ammonia on the adsorbents,

respectively. When tests are performed in the presence of water, a first increase in ammonia concentration is observed which then levels off at about 5 ppm for HKUST-1 and for the composites (especially MG-1-EM and MG-2-EM samples). Then ammonia concentration increases more rapidly. The variations in the features of the breakthrough curves between moist and dry conditions suggest different mechanisms of adsorption. The first increase in the ammonia concentration on the breakthrough curves in moist conditions might be due to a competition for adsorption between water and ammonia molecules since both are known to bind the copper sites of HKUST-1.[7, 21] Indeed, at the beginning, if water molecules tend to bind preferentially to the metallic centers, some ammonia molecules might not find any available sites to coordinate to and are thus released in the outlet stream. Then some quasi-equilibrium is reached and it allows the adsorption of ammonia which explains the "slowdown" in the increase in the ammonia concentration. Moreover, based on the shape of the desorption curves in moist conditions, it seems that ammonia interactions with the adsorbents are weaker than in dry conditions. Finally, we observe in both dry and moist conditions, that GO has breakthrough and desorption curves steeper than the ones of HKUST-1 and the composites. This indicates faster kinetics of interactions between ammonia and the adsorbent as well as a stronger retention of the molecules on the adsorbent's surface.

On the basis of the breakthrough capacities listed in Table 1, HKUST-1 appears as a good adsorbent of ammonia and exhibits a better performance in moist conditions than in dry conditions. The values found in our study are in the range of the ones reported by Peterson and coworkers (112 mg/g in dry conditions and 151 mg/g in moist conditions)[21]. Nevertheless, it has to be mentioned that the exact experimental conditions and structure of the adsorbent (flow rate, size/mass of the bed as well as the porosity of the initial MOF) were different. Unlike HKUST-1, GO shows a better capacity in dry conditions, an effect which has already been reported by Seredych and Bandosz.[34] The capacities of the composites MG-

1, MG-2 and MG-3, in dry conditions, are higher than those for the parent materials. For these three samples, the adsorption capacity increases with the content of GO from 128 mg/g to 149 mg/g. On the contrary, MG-4 and MG-5 exhibit a lower adsorption capacity than HKUST-1 and a decrease in their performance is noticed as the amount of GO increases. Overall, HKUST-1 and the composites have adsorption capacities well above the ones obtained with virgin activated carbons (between about 1 and 20 mg/g).[15] To our best knowledge, the performance of the composites exceeds the ones reported so far in the literature for various adsorbents. Examples of these adsorbents are modified activated carbons, silica gel, polymeric resins, and graphite oxide for which the highest adsorption capacities reported range from about 40 mg/g to 100 mg/g.[6, 8, 10, 34] It is interesting to compare all these values to the adsorption capacities determined assuming the physical mixture between the two components of the composites. More precisely, the latter capacities ("hypothetical capacities") were calculated as detailed in Equation (1).

$$A_{composite} = A_{GO} \times wt\%_{GO} + A_{HKUST-1} \times wt\%_{HKUST-1} \quad (1)$$

In Eq (1), "A_i" refers to the adsorption capacity (in mg/g) of the compound "i".

As seen from Table 1, the measured breakthrough capacities are always higher than the "hypothetical" ones except for MG-4 and MG-5 run in dry conditions. This suggests that except for the two latter materials, a synergetic effect occurs between the components of the composites. Two phenomena can explain this effect. The first one is the presence of increased dispersive forces in the composites owing to the presence of graphene layers, as already observed with MOF-5/GO composites.[23, 24] The second one is linked to the increased porosity of the composites compared to the parent materials as described in Ref [31]. A bar plot showing the difference between the measure adsorption capacity and the hypothetical one in in dry and moist conditions is presented in Figure 2. When positive, this difference indicates an improvement. Overall, the improvement is better pronounced in the moist conditions than

in the dry conditions. It has been shown in a previous study[31] that the surface area of MG-1, MG-2 and MG-3 was about 10% higher than the one of HKUST-1 (between 8 and 15% increase for the volume of micropores). Owing to this enhanced porosity, more space is available in the composites for water to be adsorbed when tests are performed in the presence of humidity. Ammonia is highly water-soluble which favors its adsorption when moisture is present in the system. Indeed, in such systems, a water film forms on the pore walls of the adsorbent and ammonia can then dissolve in that film. The higher the amount of water adsorbed, the higher the amount of ammonia retained by dissolution.

An increase in the amount of water adsorbed causes that the composites can adsorb more ammonia via its dissolution in the water film than can the parent materials. Obviously, this effect cannot be observed in dry conditions since water is absent in the system. In this case, only the effect of the increased dispersive forces and additional porosity can be considered. As one can see on Figure 2, in both experimental conditions (dry and moist), the improvement first increases with an increase in the amount of GO and then decreases when this content is more than 36 wt% (MG-4) for the dry conditions and 18 wt% (MG-3) for the moist conditions. This trend is in agreement with the one reported for the parameters of the porous structure for the materials studied.[31] Indeed, as briefly mentioned above, MG-1, -2, and -3 exhibit a higher surface area and volume of pores than HKUST-1, whereas for MG-4 and -5, these two quantities decreased. This trend is attributed to the fact that as the GO content increases, a maximization of the pore space can be reached. However, for too high GO contents, the formation of the MOF units in the composites becomes more difficult and distortion of the MOF structure occurs. The observed trend in adsorption capacity supports the hypothesis that the increased porosity and dispersive forces of the composites are responsible for the enhancement in the ammonia retention. Besides, signs of increased physical forces on these composites have been reported[31] where enhanced hydrogen

adsorption was measured compared to that of the parent materials. Since hydrogen is not soluble in water and likely does not react with MOF structure, the enhanced retention must be related to physisorption.

It is important to mention that, unlike in the studies reported in the literature on the adsorption of ammonia on HKUST-1,[8, 21] two changes of color of the bed, and not only one, were noticed during the breakthrough tests on HKUST-1 and on the composites. The first color change (from dark blue to deep sky blue) appeared much faster in the moist conditions than in the dry conditions. For both conditions, the second color change (from deep sky blue to Maya blue) was slower than the first change of color. The tints observed were slightly greener (teal) with the composites compared to HKUST-1 alone. Intuitively, the first change of color could be attributed to the binding of ammonia (dry conditions) or water/ammonia (moist conditions) to the copper sites. The second change of color could then originate from the formation of a new complex resulting from ammonia adsorption. A first thought is the formation of the well-known "Schweizer's reagent". This complex, whose formula is $Cu(NH_3)_4(H_2O)_2^{2+}$, has been evidenced by Peterson and coworkers as the final product of ammonia adsorption on HKUST-1 in moist conditions.[21] In our case, the presence of this complex seems unlikely since its color (deep blue) does not correspond to the one we observed. Even when the exhausted samples were immersed in water, no deep blue color was noticed.

Figure 3 visualizes all sites for ammonia adsorption in our composites before complexation with the MOF units occurs (described later). So far, two sites of adsorption have been evidenced. One is the new pore space at the interface MOF/GO where the dispersive forces are enhanced (see Figure 3, site 1). This site is responsible for the enhanced adsorption capacities measured compared to the hypothetical ones. The second site of adsorption

corresponds to the copper (see Figure 3, site 2). This latter site is evidenced by the first change of color mentioned above.

To understand the mechanisms of retention in more details and explain the second change of color of the MOF-based adsorbents, the exhausted materials run in dry and moist conditions have to be analyzed, and the results of these analyses should be compared to the ones obtained for the initial samples. Since a detailed characterization of these initial materials is reported in ref 31, only some of the features of these samples are reintroduced here to allow a better understanding of the mechanisms. Moreover, in order to distinguish between the effect of ammonia retention on the structure of the materials and the influence of water adsorption (for experiments run in moist air), HKUST-1 and the composites were exposed to a flow of humid air only for the same period of time as for the breakthrough/desorption tests. The samples were then analyzed in the same way as the ones exposed to ammonia. Comparison of the results can throw some light on the adsorption process(es).

Changes in the X-ray diffraction patterns of the materials exposed to ammonia are presented in Figure 4. Ammonia adsorption leads to a decrease in the interlayer distance of GO in both dry and moist conditions, as shown by the shift of the single peak toward higher 2Θ values. This phenomenon has already been evidenced and explained in the literature.[36] Briefly, it is caused by the reaction of ammonia with the functional groups present in the interlayer space of GO. Indeed, the ring-opening caused by the reaction of epoxy groups with ammonia and the cleavage of the C−S bond (in sulfonic groups attached to the graphene layers) due to the action of the superoxide ions were shown to lead to a more ordered staking of the graphene layers and thus a decrease of the interlayer distance.[36] Almost all the peaks on the diffraction patterns of HKUST-1 and the composites, which are characteristic of the MOF structure, disappear after ammonia adsorption in dry conditions. This indicates that the

HKUST-1 component has lost, at least partially, its crystalline structure to form one or more amorphous compounds. This is in agreement with the findings of Peterson and co-workers.(21) Unlike on the diffraction patterns for HKUST-1, MG-2, and MG-3 samples run in dry conditions, in moist conditions, most peaks remain after ammonia adsorption, but their intensities significantly decreased. It seems that despite the larger amount of ammonia adsorbed in moist conditions, some part of the HKUST-1 structure remains preserved. This can be explained by the fact that a significant part of the ammonia adsorbed was retained by dissolution in the water film and consequently did not react with the MOF structure. This hypothesis is supported by the shape of the desorption curves described above, indicating that a significant part of NH_3 was only weakly retained on the materials (HKUST-1 and composites). As seen in Figure 3, when the materials are exposed to humidity only, the X-ray diffraction patterns are mostly preserved with a decrease in the intensity of the peaks. This suggests that water, even though it is not supposed to lead to the decomposition of HKUST-1 structure in ambient conditions, caused some distortion in the materials at high humidity levels.

The FT-IR spectra of the materials before and after ammonia adsorption are reported in Figure 5. Several new features are observed for the exhausted samples. In the case of GO-ED and GO-EM, a new band at ~1430 cm^{-1} is seen and assigned to N-H vibration in NH_4^+.[37] The broad overlapping bands between 3100 and 3700 cm^{-1} are attributed to the vibrations of O-H (from phenol) and N-H (from NH_4^+, NH_3 and NH_2).[38-39] The other changes in the spectra of GO after exposure to ammonia are related to the modifications in the surface groups of GO due to their reaction with NH_3.[36] Briefly, a decrease in the intensity of the band at 1230 cm^{-1} is due to the reaction of ammonia with the epoxy groups and/or the oxidation of the sulfonic groups into sulfates. The broadening of the band at 1630 cm^{-1} can be assigned to O-H vibration formed by reaction of the epoxy groups with ammonia and/or N-H vibrations in

ammonia or amine. For HKUST-1 and the composites, new bands are observed at ~1620, 1260 and 1210 cm^{-1}. This is accompanied by a broadening of the bands at 1450, 1370 and 730 cm^{-1} and an increase in the intensity of the band at ~1560 cm^{-1}. Moreover, the thin band at ~1620 cm^{-1} "replaces" the larger one at 1645 cm^{-1}. All these features are even more pronounced for samples run in moist conditions. For the latter materials (except MG-5-EM), two bands at ~ 3350 and 3190 cm^{-1} appear and are attributed to ammonia and water vibrations.[37, 38] The absence of these bands in dry conditions is in agreement with the lower adsorption capacities in those cases as well as with the absence (or at least the lower content) of water in the system. An increase in the intensity of the band at ~1560 cm^{-1} must be related to a change in the coordination of the carboxylate ligands from BTC.[40] Moreover, based on the appearance of the thin band at ~ 1620 cm^{-1} and the ones at ~1260 and 1210 cm^{-1}, as well as the broadening of the bands at 1370 and 1450 cm^{-1}, the spectra tend to look as the one reported for BTC alone.[41] Besides, the absence of the band at ~1720 cm^{-1} excludes the presence of the acidic form of BTC.[42] Based on all these observations, it is thus hypothesized that, during ammonia adsorption, the carboxylate groups from BTC react with ammonia to form $(NH_4)_3BTC$. When the samples are exposed to moist air only (Figure 4~~5~~C), no significant changes are observed except in the range related to the carboxylate groups (1650-1300 cm^{-1}). This indicates variations in the coordination of the ligands to the copper sites. We link this to the distortion caused by water in the copper-BTC bridging. This is in agreement with the X-ray diffraction data for which a decrease in the intensity of the peaks of the HKUST-1 component was observed for all samples exposed to humid air only.

DTG curves obtained from the thermal analyses are presented in Figure 6 for all the materials tested. For the initial HKUST-1 and composite samples, three main peaks can be observed: one at about 100 °C corresponding to the solvent removal, another at about 300 °C related to the removal of the water of crystallization, and finally one at 350 °C when the

decomposition of the BTC unit occurs.[31] In dry conditions, two broad peaks can be seen before the decomposition of the HKUST-1 structure: a first one between 30 and 110 °C (centered at 70 °C) and a second one at 110−270 °C (highest intensity between 180 and 230 °C). The latter peak can be related to the removal of strongly adsorbed ammonia (on the copper sites, via hydrogen bonding to the oxygen atoms of the carboxylate ligands or from (NH4)3BTC) and/or to the release of water from $Cu(OH)_2$.[43, 44] The first peak is linked to the removal of ammonia physically adsorbed in small pores. A broad peak revealed between 270 and 400 °C is likely related to the decomposition of BTC. However, the different shoulders present at this temperature range (at 320, 340, and 360 °C) on MG-1, MG-2, and MG-3 samples suggest that more than one compound containing BTC is present. These compounds might include HKUST-1, $Cu(NH_3)_2BTC_{2/3}$, and $(NH_4)_3BTC$. In moist conditions, a first peak at about 90 °C is observed and assigned to the removal of physically adsorbed water. The latter peak comes with a small shoulder at 115 °C which is better seen for HKUST-1 and MG-1 samples. That peak represents the removal of weakly adsorbed ammonia/ammonia dissolved in water. As for dry conditions, the continuous weight loss between 110 and 270 °C is related to the removal of strongly adsorbed ammonia and/or the release of water from $Cu(OH)_2$. A broad peak at 325 °C is also observed. Unlike the curves in dry conditions, the shoulders of the latter peak are less visible. A great part of the HKUST-1 component has probably already decomposed to form $(NH_4)_3BTC$. A peak at 40 °C is observed on the DTG curve of MG-2-EM only. So far, we cannot propose any explanation for this peculiar feature. When the materials are exposed to moist air only, the DTG curves are not significantly modified. However, the shape of the peak related to the decomposition of the HKUST-1 structure is changed, suggesting some changes/distortion in the structure caused by water adsorption. This is in agreement with the X-ray diffraction and FT-IR data. A broad peak is observed at 100 °C and assigned to the removal of water. Similar conditions in terms of

humidity levels and duration of the tests were used to run the ammonia adsorption in moist conditions and to expose the materials to moist air only. Despite this, the amount of water desorbed at 100 °C is greater in the latter case. This suggests the preferred adsorption of ammonia on the materials compared to the one of water when the two molecules are present in the system. This is supported by the fact that when samples were subjected to a step of prehumidification before the breakthrough test in dry conditions (see Materials and Methods section for description of the tests), the breakthrough capacities obtained were similar to the ones found in dry conditions (data are not presented here). Moreover, the results of the analyses of the exhausted samples after the prehumidification (X-ray, FT-IR, thermal analyses) lead to results similar to the ones obtained in dry conditions (data are not presented here).

After exposure to ammonia in dry conditions, selected samples (HKUST-1, MG-1 and MG-3) were analyzed by nitrogen adsorption to assess the effect of ammonia retention on the porosity of the samples. The exhausted samples were found non porous. This supports the collapse of the MOF structure and the complexation processes described above.

Conclusions

The MOF/graphene composites exhibit much better ammonia adsorption capacities than the ones calculated for the physical mixture of HKUST-1 and GO. This indicates the presence of a synergetic effect between the two components. We link it to the increase in porosity and the enhanced dispersive forces in the composites compared to the parent materials. In addition to its physical adsorption, ammonia is adsorbed via binding to the copper sites in HKUST-1 (formation if $Cu(NH_3)_2BTC_{2/3}$) and then progressively via reaction with the MOF component. It is suggested that this reaction leads to the formation of $Cu(OH)_2$ and $(NH_4)_3BTC$. These two steps of adsorption (binding and reaction) are visible through two successive changes of

color of the adsorbents during the breakthrough tests. The amount of ammonia adsorbed is higher in moist conditions than in dry conditions owing to its dissolution in the water film present in materials' pores. The improvement in terms of ammonia adsorption capacity of these composites supports the results obtained previously for MOF-5/GO composites. However, the materials reported here have the advantage to be water stable and are thus better adapted to environmental applications than the MOF-5/GO composites which collapsed in presence of moisture.

Acknowledgements

This study was supported by the ARO (Army Research Office) grant W911NF-05-1-0537 and NSF collaborative grant 0754945/0754979.

References

(1) Loureiro, J. M.; Kartel, M. T.; Loureiro, J. M. *Combined and hybrid adsorbents: Fundamentals and Applications*; Springer-Verlag: New York, 2006.

(2) Schuth, F.; Sing, K. S. W.; Weitkamp, J. *Handbook of porous solids*; John Wiley and Sons: New York, 2008.

(3) Yeung, C. S.; Liu, L. V.; Wang, Y. A. *J. Phys. Chem. C* **2008**, *112*, 7401-7411.

(4) Coasne, B.; Galarneau, A.; Di Renze, F.; Pellenq, R. J. M. *Langmuir* **2006**, *22*, 11097-11105.

(5) Pagans, E.; Font, X.; Sanchew, A. Chem. Eng. J. **2005**, *113*, 105-110.

(6) Helminem, J.; Helenius, J.; Paatero, E. *Chem. Eng. Data* **2001**, *46*, 391-399.

(7) Britt, D.; Tranchemontagne, D.; Yaghi, O. M. *Proc. Nat. Acad. Sci. U.S.A.* **2008**, *105*, 11623-11627.

(8) Seredych, M.; Petit, C.; Tamashausky, A. V.; Bandosz, T. J. Carbon **2009**, *47*, 445-456.

(9) Li, J.-R.; Kuppler, R. J.; Zhou, H.-C. Chem. Soc. Rev. **2009**, *38*, 1477-1504.

(10) Petit, C.; Karwacki, C.; Peterson, G.; Bandosz, T. J. *J. Phys. Chem. C* **2007**, *111*, 12705-12714.

(11) Thompson, J. C. *Phys. Rev. A* **1971**, *4*, 802-804.

(12) Spencer, W. B.; Amberg, C. H.; Beebe, R. A. *J. Phys. Chem.* **1968**, *62*, 719-723.

(13) Overstreet, R.; Giauque, W. F. *J. Am. Chem. Soc.* **1937**, *59*, 254-259.

(14) Stoeckli, F.; Guillot, A.; Slasli, A. M. *Carbon* **2004**, *42*, 1619-1624.

(15) Bandosz, T. J.; Petit, C. *J. Colloid Interf. Sci.* **2009**, *338*, 329-345.

(16) Ferey, G. *Chem. Soc. Rev.* **2008**, *37*, 191-214.

(17) Wright, P. A. *Microporous frameworks solids*; Springer-Verlag: New York, 2007.

(18) James, S. L. *Chem. Soc. Rev.* **2003**, *32*, 276-288.

(19) Czaja, A. U.; Trukhan, N.; Muller, U. Chem. Soc. Rev. **2009**, *38*, 1284-1293.

(20) Muller, U.; Schubert, M. M.; Yaghi, O. M. In *Handbook of Heterogeneous Catalysis*, Ertl, G., Knozinger, H., Schuth, F., Weitkamp, J., Eds.; John Wiley and Sons: New York, 2008; p. 247-262.

(21) Peterson, G. W.; Wagner, G. W.; Balboa, A.; Mahle, J.; Sewell, T.; Karwacki, C. J. *J. Phys. Chem. C* **2009**, *113*, 13906-13917.

(22) Chui, S. S.-Y.; Lo, S. M.-F.; Charmant, J. P. H.; Orpen, A. G.; Williams, I. D. Science **1999**, *283*, 1148-1150.

(23) Petit, C.; Bandosz, T. J.*Adv. Funct. Mater.* **2010**, *20*, 111-118.

(24) Petit, C.; Bandosz, T. J. *Adv. Mater.* **2009**, *21*, 4753-4757.

(25) Kaye, S. S.; Dailly, A.; Yaghi, O. M.; Long, J. R. *J. Am. Chem. Soc.* **2007**, *129*, 14176-14177.

(26) Prestipino, C.; Regli, L.; Vitillo, J. G.; Bonino, F.; Damin, A.; Lamberti, C.; Zecchina, A.; Solari, P. L.; Kongshaug, K. O.; Bordiga, S. *Chem. Mater.* **2006**, *18*, 1337-1346.

(27) Cheng, Y.; Kondo, A.; Noguchi, H.; Kajiro, H.; Urita, K.; Ohba, T.; Kaneko, K.; Kanoh, H. *Langmuir* **2009**, *25*, 4510-4513.

(28) Gu, J. Z.; Lu, W. G.; Jiang, L.; Zhou, H. C.; Lu, T. B. *Inorg. Chem.* **2007**, *46*, 5835-5837.

(29) Kusgens, P.; Rose, M.; Senkovska, I.; Frode, H.; Henschel, A.; Siegle, S.; Kaskel, S. *Microporous Mesoporous Mater.* **2009**, *120*, 325-330.

(30) Park, K. S.; Ni, Z.; Cote, A. P.; Choi, J. Y.; Huang, R.; Uribe-Romo, F. J.; Chae, H. K.; O'Keeffe, M.; Yaghi, O. M. *Proc. Nat. Acad. Sci. U.S.A.* **2006**, *103*, 10186-10191.

(31) Petit, C.; Burress, J.; Bandosz, T. J. *Phys. Chem. Chem. Phys*. Submitted.

(32) Pauling, L. In *General Chemistry*, Linus, P, Ed.; Dover Publications: Mineola, New York, 1988; pp. 654-678.

(33) A. R. Millward, O. M. Yaghi, *J. Am. Chem. Soc.* **2005**, *127*, 17998-17999.

(34) Seredych, M.; Bandosz, T. J. *J. Phys. Chem. C* **2007**, *111*, 15596–15604.

(35) Dubinin, M. M. In *Chemistry and Physics of Carbon*, Walker, P. L., Ed.; M. Dekker, New York, 1966; pp. 51-120.

(36) Petit, C.; Seredych, M.; Bandosz, T. J. *J. Mater. Chem.* **2009**, *19*, 9176-9185.

(37) Zawadszki, J.; Wisniewski, M. Carbon **2003**, *41*, 2257-2267.

(38) Weast, R. C.; Astle, M. J. In *Handbook of Chemistry and Physics*, Weast, R. C., Astle, M. J., Eds.; CRC Press: Boca Raton, Florida, 1981, 62nd edition.

(39) Onida, B.; Gabelica, Z.; Lourenco, J.; Garrone, E. *J. Phys. Chem.* **1996**, *100*, 11072-11079.

(40) Nakamoto, K. In *Infrared and Raman spectra of inorganic and coordination compounds*, Nakamoto, K., Ed.; John Wiley and Sons: New York, 2009; Vol. B, pp. 62-67.

(41) Shi, N.; Yin, G.; Han, M.; Jiang, L.; Xu, Z. *Chem. Eur. J.* **2008**, *14*, 6255-6259.

(42) Seo, Y. K.; Hundal, G.; Jang, I. T.; Hwang, Y. K.; Jun, C. H.; Chang, J. S. *Microporous Mesoporous Mater.* **2009**, *119*, 331-337.

(43) Ramamurthy, P.; Secco, E. A. *Can. J. Chem.* **1969**, *47*, 2303-2304.

(44) Liu, N.; Wu, D.; Wu, H.; Luo, F. J. Chen, *Solid State Sci.* **2008**, *10*, 1049-1055.

CAPTIONS TO THE TABLES

Table 1. Ammonia breakthrough capacities (measured and recalculated) and initial surface pH values for the parent and composites materials.

CAPTIONS TO THE FIGURES

Figure 1. Ammonia breakthrough curves and desorption curves for the parent materials and the composites in (A) dry and, (B) moist conditions.

Figure 2. Difference between the measured adsorption capacities and the ones calculated for the physical mixture for all the composites, in both dry and moist conditions.

Figure 3. Visualization of two sites of ammonia adsorption in the composites with (1) physisorption at the interface between graphene layers and MOF units and (2) binding to the copper centers. Ammonia molecule is represented by the dark gray circles.

Figure 4. X-ray diffraction patterns for the parent materials and the composites before (black lines) and after (grey lines) exposure to ammonia in (A) dry and (B) moist conditions, and after exposure to moisture only (C).

Figure 5. FT-IR spectra for the parent materials and the composites before (dashed lines) and after (plain lines) exposure to ammonia in (A) dry and (B) moist conditions, and after exposure to moisture only (C).

Figure 6. DTG curves for the parent materials and the composites before (black lines) and after (grey lines) exposure to ammonia in (A) dry and (B) moist conditions, and after exposure to moisture only (C).

Table 1. Ammonia breakthrough capacities (measured and recalculated) and initial surface pH values for the parent and composites materials.

Sample	NH_3 breakthrough capacity [mg/g of carbon]	Hypothetical NH_3 breakthrough capacity [mg/g of carbon]	pH initial
GO-ED	45	-	2.47
GO-EM	33	-	2.47
HKUST-1-ED	115	-	4.19
HKUST-1-EM	172	-	4.19
MG-1-ED	128	111	4.22
MG-1-EM	200	165	4.22
MG-2-ED	131	108	4.34
MG-2-EM	231	159	4.34
MG-3-ED	149	102	4.45
MG-3-EM	182	147	4.45
MG-4-ED	87	88	4.23
MG-4-EM	147	119	4.23
MG-5-ED	70	81	4.32
MG-5-EM	123	108	4.32

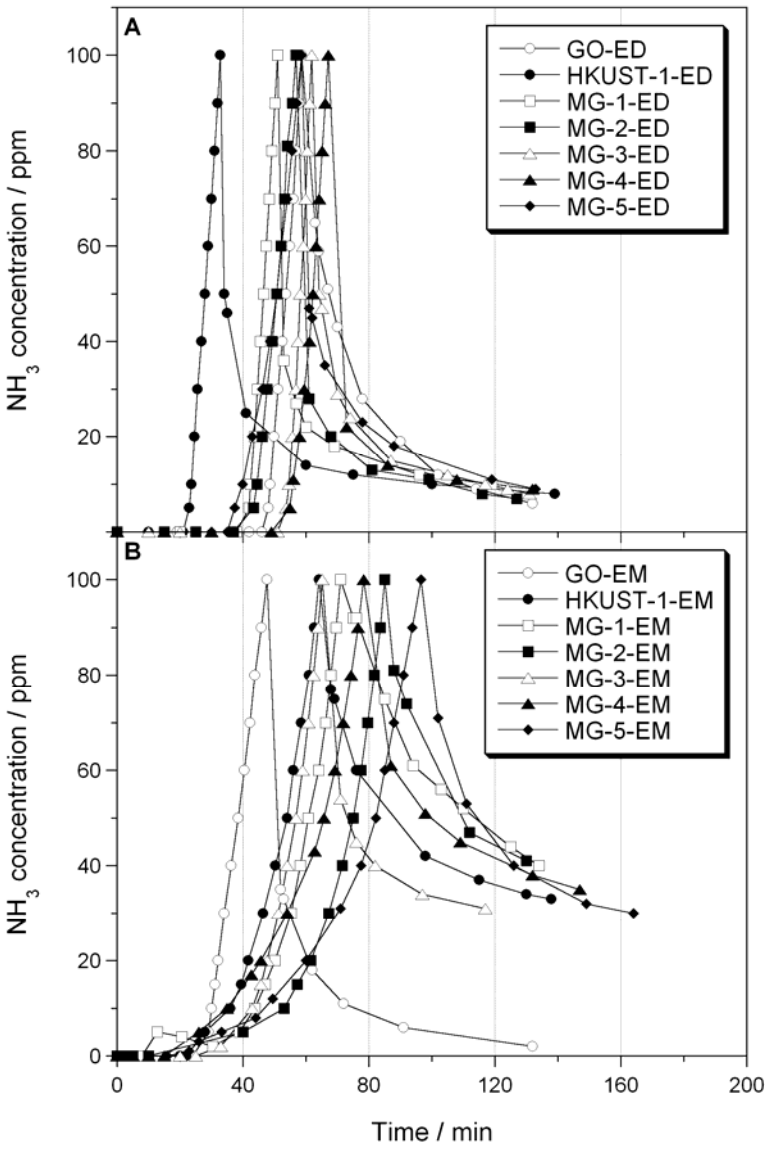

Figure 1. Ammonia breakthrough curves and desorption curves for the parent materials and the composites in (A) dry and, (B) moist conditions.

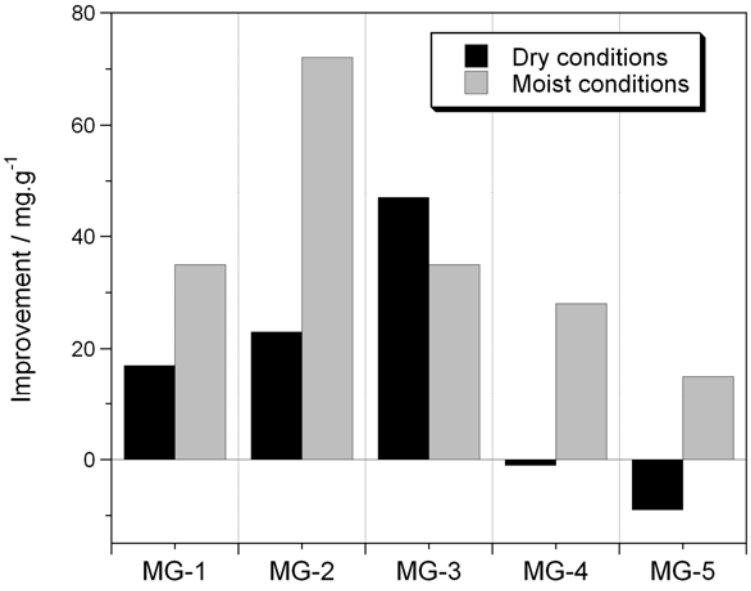

Figure 2. Difference between the measured adsorption capacities and the ones calculated for the physical mixture for all the composites, in both dry and moist conditions.

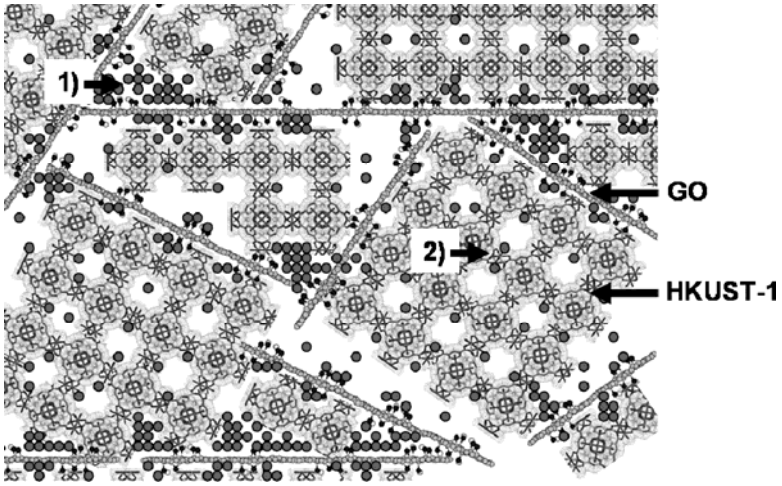

Figure 3. Visualization of two sites of ammonia adsorption in the composites with (1) physisorption at the interface between graphene layers and MOF units and (2) binding to the copper centers. Ammonia molecule is represented by the dark gray circles.

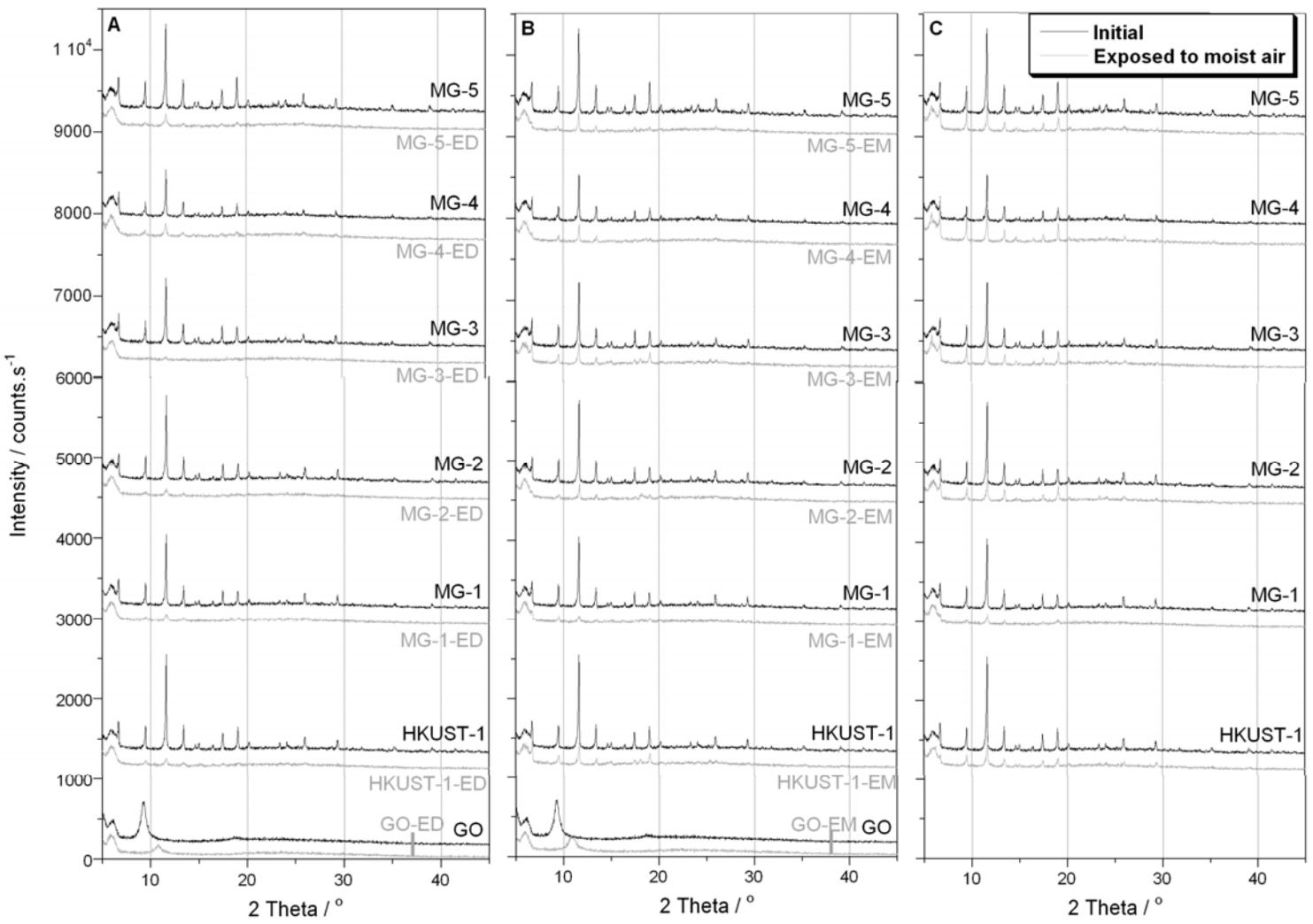

Figure 4. X-ray diffraction patterns for the parent materials and the composites before (black lines) and after (grey lines) exposure to ammonia in (A) dry and (B) moist conditions, and after exposure to moisture only (C).

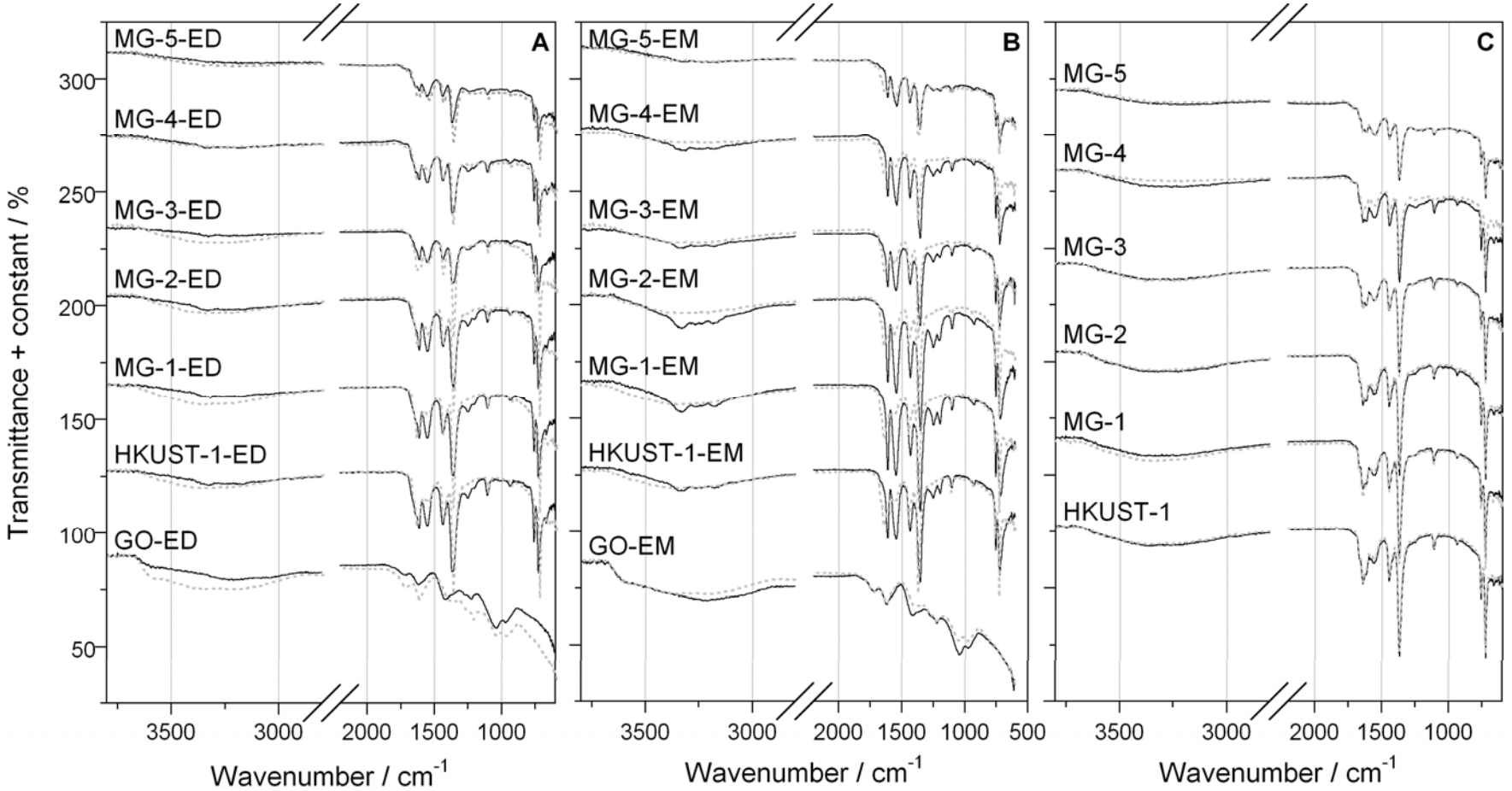

Figure 5. FT-IR spectra for the parent materials and the composites before (dashed lines) and after (plain lines) exposure to ammonia in (A) dry and (B) moist conditions, and after exposure to moisture only (C).

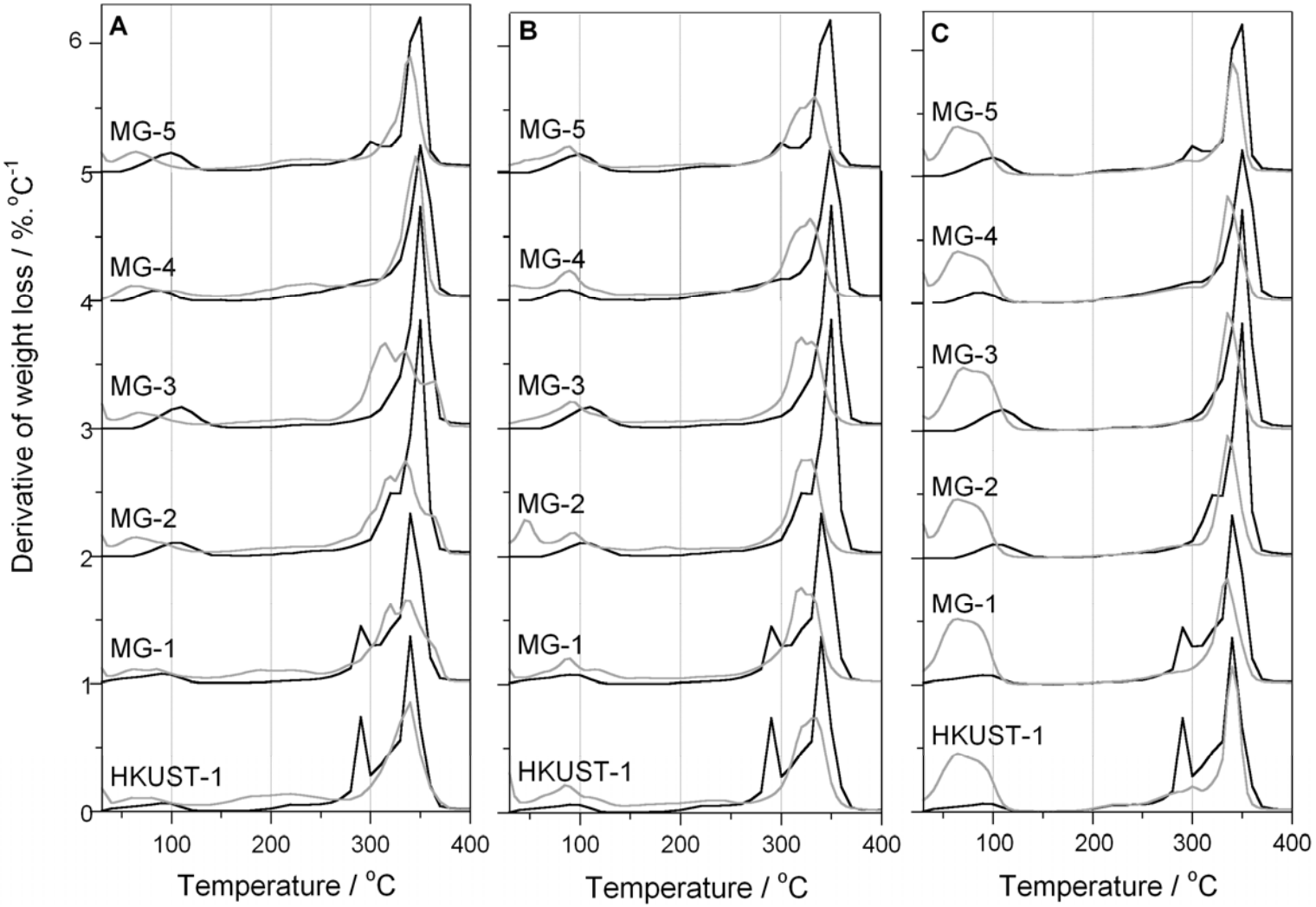

Figure 6. DTG curves for the parent materials and the composites before (black lines) and after (grey lines) exposure to ammonia in (A) dry and (B) moist conditions, and after exposure to moisture only (C).

Table of content only

C. Petit, B. Beacom, T. J. Bandosz*

Reactive adsorption of ammonia on Cu-based MOF /graphene composites